npg

The bromodomain protein BRD4 regulates the KEAP1/NRF2-dependent oxidative stress response

M Hussong[1,2], ST Börno[1], M Kerick[1], A Wunderlich[1], A Franz[1,2], H Sültmann[3], B Timmermann[4], H Lehrach[1], M Hirsch-Kauffmann[1] and MR Schweiger*[,1,5]

The epigenetic sensor BRD4 (bromodomain protein 4) is a potent target for anti-cancer therapies. To study the transcriptional impact of BRD4 in cancer, we generated an expression signature of BRD4 knockdown cells and found oxidative stress response genes significantly enriched. We integrated the RNA-Seq results with DNA-binding sites of BRD4 generated by chromatin immunoprecipitations, correlated these with gene expressions from human prostate cancers and identified 21 top BRD4 candidate genes among which the oxidative stress pathway genes KEAP1, SESN3 and HDAC6 are represented. Knock down of BRD4 or treatment with the BRD4 inhibitor JQ1 resulted in decreased reactive oxygen species (ROS) production and increased cell viability under H_2O_2 exposure. Consistently, a deregulation of BRD4 diminished the KEAP1/NRF2 axis and led to a disturbed regulation of the inducible heme oxygenase 1 (HMOX1). Without exogenous stress induction, we also found BRD4 directly targeting the HMOX1 promoter over the SP1-binding sites. Our findings provide insight into the transcriptional regulatory network of BRD4 and highlight BRD4 as signal transducer of the cellular response to oxidative stress.
Cell Death and Disease (2014) **5,** e1195; doi:10.1038/cddis.2014.157; published online 24 April 2014
Subject Category: Cancer

The permanent exposure of organisms to environmental changes requires a variety of cellular adaption processes. The response of cells to exogenous stressors, such as inflammation, xenobiotics, heat or ionizing radiation, is regulated by multiple stress response pathways helping to maintain or rearrange cellular homeostasis or to repair stress-induced damage. The antioxidant defense following oxidative stress injury activates signaling pathways such as the Nf-κB[1] and the Kelch-like ECH-associated protein 1 (KEAP1)/NRF2 (nuclear factor, erythroid 2-like 2, NFE2L2) pathway[2] that can promote cell survival or apoptosis.

Within the KEAP1/NRF2 pathway, KEAP1 senses electrophilic and oxidative stress and functions as a substrate adapter protein for the E3 ubiquitin ligase complex. The transcription factor NRF2, when bound to KEAP1, is a highly unstable protein that is polyubiquitinated and targeted for selective degradation via the ubiquitin proteasome pathway.[2–4] Upon stress, induced by diverse stimuli – including reactive oxygen species (ROS), heme or metalloporphyrins – reactive cysteine residues of KEAP1 become modified, which alters the structural integrity of the KEAP1–Cul3 E3 ligase complex. As a result, NRF2 escapes from KEAP1-dependent degradation and accumulates in the nucleus.[2,5,6] Here, NRF2 acts as transcriptional activator of cytoprotective genes.

NRF2-regulated genes are involved in glutathione synthesis, such as glutathione S-transferase Pi[7,8] and in the elimination of ROS, facilitated by superoxide dismutases (SOD) and heme oxygenase 1 (HMOX1).[9] In humans, the KEAP1/NRF2 pathway is frequently disrupted in lung cancer.[10–12]

We have found the KEAP1/NRF2 stress response to be regulated by bromodomain-containing protein 4 (BRD4). Early on, the bromodomain protein BRD4 has been implicated in transcriptional regulation processes.[13–15] BRD4 interacts with the positive transcriptional elongation factor b and promotes the phosphorylation of RNA polymerase II.[16,17] Recent work has also discovered that BRD4 binds to the so-called 'super-enhancers'.[18] Super-enhancers are characterized by a large size, high transcription factor density and content and increased binding of the Mediator complex.[19] In multiple myeloma (MM), for example, super-enhancers are approximately 15-fold larger and have a 16–18-fold increase in Mediator and BRD4 binding in comparison to regular enhancers. They are also frequently associated with *MYC* and other tumor-specific genes.[18]

These mechanisms might all contribute to the discovery of BRD4 as a valuable drug target in many tumor entities, including leukemia, lung cancer, MM and melanoma.[20–23] However, to date the exact mechanism of BRD4 inhibition as a

powerful anti-cancer treatment is still unclear. Here, we show that BRD4 is a regulator of KEAP1 transcription. Downstream of KEAP1, NRF2 coordinates the induction of HMOX1 as well as other oxidative stress-related genes, and alterations in BRD4 expression result in a de-regulated oxidative stress response answer. This regulatory function is disrupted in prostate cancer and thus might have a central role in malignant processes.

Results

Identification of BRD4-regulated genes in prostate cancer. In a systems biological approach, we have previously generated gene expression profiles from 48 normal and 47 tumor prostate tumor tissue samples.[24] Here, gene expression analyses of BRD4 revealed a significant increase of *BRD4* in our prostate tumor samples (Supplementary Figure S1a). To investigate which BRD4 target genes are most significantly de-regulated in cancer, we first aimed to identify BRD4 target genes. We therefore generated RNA-Seq expression data of two *BRD4* knockdown experiments in HEK293T cells and integrated it with BRD4 DNA-binding results gained by two BRD4 chromatin immunoprecipitation (ChIP)-Seq experiments (Figure 1a). In gene expression analyses, we identified 1844 genes significantly differentially regulated (log2FC > ± 0.4) in both RNA-Seqs with mean log2FC > ± 0.5 (Supplementary Table S1). Of these, 970 were upregulated – and 887 were downregulated. We focused our further analyses on the 887 downregulated genes to elucidate a potential direct transcriptional activating role of BRD4. With BRD4 ChIP experiments, we identified 1885 significant BRD4-binding site peaks (FDR < 5%) when combining enriched peaks of our two ChIP-Seq experiments. We annotated genes with a BRD4-binding site within 0.5 kb of the transcription start site (TSS) (Supplementary Table S2). Integration of both gene lists – the data obtained by the RNA-Seq and ChIP-Seq experiments – resulted in 52 commonly activated genes of BRD4, now considered as our top candidate target genes (Supplementary Table S3).

Further, we selected genes from our prostate tissues gene expression profiles with correlations to *BRD4* expression > 0.4 (Figure 1b). Out of our 52 BRD4 target genes, we identified 21 genes with positive correlations to *BRD4* in prostate cancer (Supplementary Table S4). We termed them cancer-relevant BRD4 target genes. Interestingly, among these, three were involved in the maintenance of physiological concentrations of intracellular ROS: *SESN3* (sestrin 3), *HDAC6* (histone deacetylase 6), and *KEAP1*. These and two additional genes (*MAPK3* and *VIM*) were validated in independent ChIP-quantitative PCR (qPCR) experiments in DU-145 prostate cancer cell lines (Figure 1c).

KEAP1 is a transcriptional target of BRD4 and a gatekeeper of the oxidative stress response in cancer. The KEAP1/NRF2 interplay, mediator of one of the major oxidative stress response pathways, is frequently disturbed by somatic mutations in many cancer entities.[12,25] We found *KEAP1* upregulated in prostate cancer and highly correlated with *BRD4* (Figure 1d and Supplementary Figure S1b). To see whether the oxidative stress response pathway in

general is affected by BRD4, we used a list of oxidative stress responsive genes (Gene Ontology, GO:0034599, 'cellular response to oxidative stress') and performed an enrichment analysis in the *BRD4* knockdown experiment (Supplementary Table S1). Indeed, we found a significant enrichment of these genes indicating a functional role of BRD4 in the defense against oxidative stress (OR = 3.9; P-value = 2.7×10^{-5}, Supplementary Table S5). Besides the KEAP1/NRF2 pathway, we also found other stress-responsive pathways affected by *BRD4* knockdown, albeit to a lower degree (Table 1).

Next, we asked which genes of the oxidative stress response were most significantly de-regulated by *BRD4* depletion. Besides transcriptional regulators, such as *PML*, *TP53* and *MDM2*, we found genes coding for enzymes of the antioxidant system, including *CAT* (catalase), *SOD2* (superoxide dismutase 2) and *GPX1* (glutathione peroxidase 1). These genes are predominant targets of NRF2[26,27] and were all significantly downregulated upon *BRD4* knockdown. This was a somewhat unexpected result, because knock down of *BRD4* decreased KEAP1 and should result in an increase of NRF2 and its target genes. Besides CAT, SOD2 and GPX1, the inducible enzyme HMOX1 is one of the best investigated targets of the NRF2/KEAP1 pathway. Although due to incongruent results not part of our initial RNA-Seq candidate list, we also found *HMOX1* de-regulated after *BRD4* knockdown by western blotting (Figure 1e) and qPCR (Supplementary Figure S2a) experiments. Thus, both – *KEAP1* as well as *HMOX1* (and other NRF2 target genes) – were significantly downregulated after BRD4 knockdown, demonstrating their dependence on BRD4.

Interestingly, when we investigated the expression levels of *BRD4*, *KEAP1*, *NRF2* and *HMOX1* in three prostate cancer cell lines (DU-145, LNCAP and PC3), we found a significant upregulation of *BRD4* and *KEAP1* and a downregulation of *NRF2* in all cell lines (Figure 1f). In contrast, *HMOX1* was upregulated in DU-145, downregulated in PC3 and not altered in LNCAP cells, again showing that a downregulation of *NRF2* not necessarily results in a low expression of HMOX1. Thus, we were now wondering whether this is also consistent after HMOX1 induction.

BRD4 knockdown increases the induction of HMOX1 after cobalt protoporphyrin (CoPP) stimulation through enhancing the NRF2 DNA-binding affinity. *HMOX1* expression is inducible by various stimuli, including metalloporphyrins, such as CoPP. Having observed that *BRD4* knockdown in unstressed cells significantly repressed *KEAP1* and *HMOX1* expression, we asked whether BRD4 influences the CoPP-mediated induction of *HMOX1*. Indeed, *BRD4* knockdown experiments in combination with CoPP induction showed that, under these conditions, a reduced *BRD4* level resulted in an elevated *HMOX1* expression in a time-dependent manner of CoPP stimulation (Figure 2a). To get further insight into the effect of BRD4 on the CoPP-mediated induction of HMOX1, we transfected cells with a BRD4 overexpression plasmid and analyzed the *HMOX1* expression after stimulation with varying concentrations of CoPP. In this case, the overexpression of BRD4 led to an attenuated activation of *HMOX1* RNA expression compared
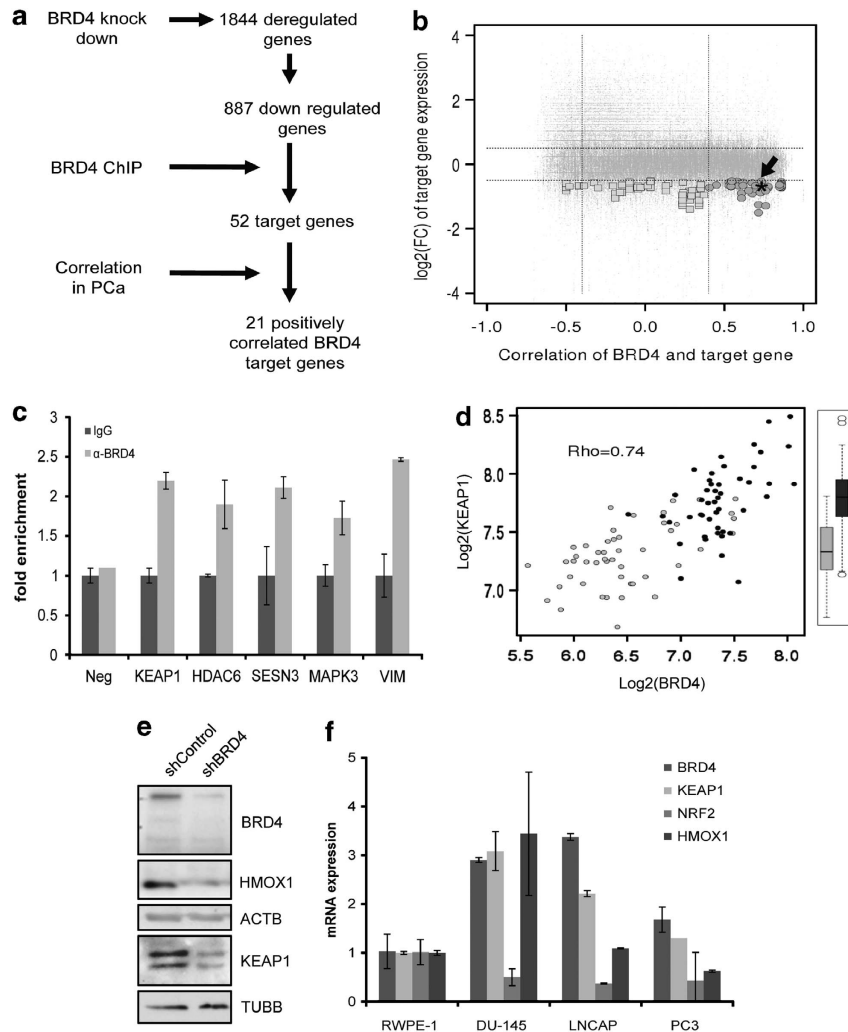
Figure 1 BRD4 target genes are significantly over-represented in prostate cancer. (**a**) Flow diagram illustrating the integration of RNA-Seq, ChIP-Seq and correlation analyses of genome-wide gene expression patterns in prostate tissues for the identification of target genes of BRD4. (**b**) Integration of differential gene expression data obtained by RNA-Seq of *BRD4* knockdown experiments and correlation data of *BRD4* in 95 primary prostate tumor and normal tissue samples. The ordinate shows the log2(ratios) of BRD4 knockdown *versus* control in HEK293T cells. The abscissa depicts the Spearman correlation values of BRD4 expression to the expression of each gene in tumor and normal prostate samples measured by gene expression arrays.[24,59] Putative *BRD4* target genes with a log2(ratio) of below − 0.4 and a mean log2(ratio) below − 0.5 in both cell line experiments (Supplementary Table S1) that we also found in our BRD4 ChIP-Seq analyses are highlighted by a square. Circles mark putative targets additionally exhibiting a positive correlation of > + 0.3 between BRD4 and the gene candidate in prostate samples. Dotted horizontal lines denote log2(ratio) values of 0.4 and − 0.4 while vertical lines represent correlation thresholds of 0.3 and − 0.3. KEAP1 is marked by an asterisk (*). (**c**) ChIP validations of BRD4 binding in DU-145 cells to the indicated promoters using region-specific primer and an intergenic NCR as negative control. (**d**) Correlation between KEAP1 and BRD4 in prostate samples (gray = normal, black = tumor; Rho = 0.74). The boxplots on the right side of the plot show the differential expressions between tumor ($n = 47$) and normal samples ($n = 48$) of KEAP1 (Mann–Whitney *P*-value $< 4.7 \times 10^{-12}$). (**e**) Western blot of BRD4, HMOX1 and KEAP1 after *BRD4* knockdown. HEK293T cells were transfected with either shBRD4 or a control shRNA (shControl) and harvested 72 h post transfection. As loading control β-actin (ACTB) and α-tubulin (TUBB) were used. (**f**) BRD4, KEAP1, NRF2 and HMOX1 mRNA expression in prostate cancer cell lines using qPCR. The expression was determined in at least two independent experiments

Table 1 Enrichment of stress response pathways in *BRD4* knockdown RNA-Seq experiments

GO number	GO name	BRD4 KD	Data set	Odds ratio	P-value
GO:0034599	Cellular response to oxidative stress	16	70	3.88	2.3×10^{-5}
GO:0006970	Osmotic stress response	11	61	2.87	3.7×10^{-3}
GO:0010038	Response to metal ion	32	285	1.66	0.01
GO:0009408	Response to heat	5	64	1.10	0.81
GO:2001020	DNA damage response	4	82	0.66	0.52
GO:0050727	Inflammatory response	27	162	2.63	3.75×10^{-5}
GO:0034976	Response to ER stress	14	135	1.50	0.18
GO:0001666	Response to hypoxia	24	255	1.35	0.18
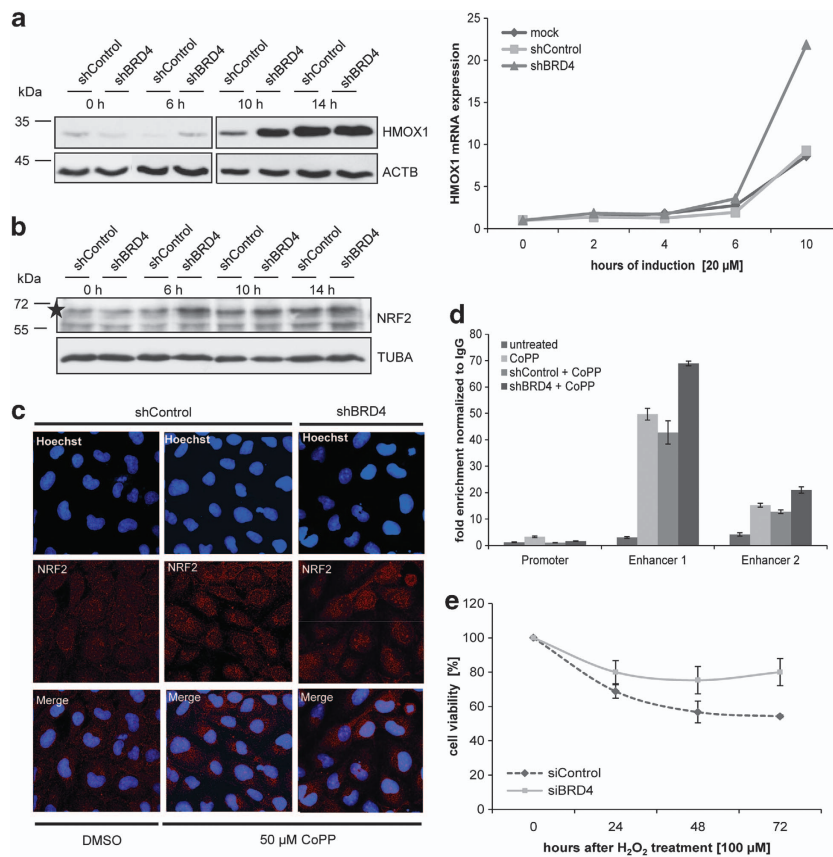
Figure 2 BRD4 regulates the stress-mediated expression of HMOX1. (**a**) HEK293T cells were transfected with either shBRD4 or shControl and stimulated with 20 μM of CoPP for 6, 10 and 14 h for western blot analysis (left) or 2, 4, 6 and 10 h for qPCRs with tubulin as reference gene (right). (**b**) Western blot analysis of the NRF2 expression after CoPP treatment. NRF2 (star) protein levels were measured after treatment with 20 μM CoPP in BRD4 knockdown cells (shBRD4) or control cells (shControl) after 6, 10 and 14 h, as indicated. Tubulin (TUBA) was used as a loading control. (**c**) Immunofluorescence of NRF2 after CoPP stimulation. WI-38 cells were transfected with either shBRD4 or a control shRNA (shControl) and treated with 50 μM CoPP or DMSO for 6 h. After 72 h, cells were stained with antibodies against NRF2 and Hoechst and examined with a confocal fluorescence microscope (LSM 510 meta, Zeiss). (**d**) ChIP analyses of the NRF2 binding to enhancer regions of the HMOX1 promoter. ShBRD4 knockdown or shControl cells were treated with 50 μM CoPP or DMSO for 6 h. The NRF2 binding to the HMOX1 promoter as well as to both enhancers was analyzed with qPCRs using region-specific primers. (**e**) Cell viability assay of BRD4 knockdown. WI-38 cells were transfected either with siBRD4 or non-targeting control siRNA. After 24 h, cells were treated with 100 μM H_2O_2 for 30 min. Cell viability was measured after 24, 48 and 72 h using the Alamar Blue reagent

with the corresponding mock control (Supplementary Figure S3a). To explore whether the enhanced induction of *HMOX1* by *BRD4* knockdown after stimulation was due to an increase in NRF2 caused by a decreased KEAP1 protein level (as already seen after BRD4 knockdown), we treated HEK293T cells ($+/-$ *BRD4* knockdown) with 20 μM CoPP and analyzed the endogenous NRF2 protein level at different time points. NRF2 increased in a time-dependent manner after CoPP induction in the control BRD4 cells, but, interestingly, NRF2 was even more increased in the *BRD4* knockdown cells after CoPP treatment (Figure 2b). The increased NRF2 level was not due to an increased transcriptional activity (Supplementary Figure S3b). As expected, we found *KEAP1* downregulated with and without stress (Supplementary Figure S3c). In addition, we found an increased nuclear accumulation of NRF2 in *BRD4* knockdown cells under CoPP treatment compared with the control cells (Figure 2c). To further investigate whether the increased NRF2 accumulation also resulted in an enhanced DNA binding of NRF2, we performed ChIP experiments in CoPP-treated and -untreated *BRD4* knockdown cells. NRF2

binds to antioxidant-responsive elements and NF-E2/Maf-recognition elements, respectively, that are mainly found in the enhancer regions E1 and E2, located $\sim$3 kb and $\sim$10 kb upstream of the transcription-initiation site.[3,28] We tested the NRF2 enrichment on both *HMOX1* enhancers as well as on the promoter region, which was used as negative control. Actually, *BRD4* reduction significantly increased NRF2 binding to both *HMOX1* enhancers after CoPP induction (Figure 2d). Further functional experiments demonstrated a low level of BRD4 to be advantageous for cells under stress: We treated control cells as well as cells with *BRD4* knockdown with hydrogen peroxide (H_2O_2) and measured cell survival over 72 h. Accordingly, cells with diminished *BRD4* expression displayed an increased cell survival upon H_2O_2 treatment compared with control cells (Figure 2e).

The BRD4 inhibitor JQ1 reduces ROS and increases cell survival upon oxidative stress. The upregulation of HMOX1 protects cells against increased levels of ROS and consequently against oxidative stress-mediated cell death. Hence, we tested whether the increased HMOX1 induction in

BRD4 knockdown resulted in a decreased ROS level and an enhanced cell survival. For these experiments, we used the bromodomain and extra-terminal (BET) inhibitor JQ1[29] and measured the expression level of *KEAP1*. Similar to the *BRD4* knockdown experiments, we found a downregulation of *KEAP1* in a dose-dependent manner upon JQ1 treatment (Figure 3a). We also measured the cell viability of cells treated with and without JQ1 under oxidative stress conditions. These experiments confirmed our observation of a decreased cell death after oxidative stress induction in cells with an inhibited *BRD4* function (Figure 3b). Next, we investigated the level of ROS in cells with diminished *BRD4* activity with and without H_2O_2 addition. We used a dihydrorhodamine 123 (DHR) flow cytometry assay and observed, after H_2O_2 treatment, a significant reduced number of cells with high levels of ROS in JQ1-treated cells compared with the dimethyl sulfoxide (DMSO) control (Figures 3c and d). Thus, the inhibition of BRD4 lowers intracellular ROS levels after exposure to stress, which might be the explanation for the increased cell viability (Figure 3b).

Furthermore, we also measured the amount of ROS in the prostate cancer cell line DU-145. As we had observed a significant upregulation of *BRD4* in DU-145 cells (Figure 1f), we expected an increased ROS production in these cells upon H_2O_2 treatment. Indeed, we detected a slight increase in ROS levels in the DU-145 cell line in comparison to the cell line RWPE-1, a cell line derived from normal prostate tissue (data not shown). Nevertheless, a treatment with JQ1 inhibitors in DU-145 cells did not result in a shift towards lower ROS concentrations. This was also mirrored by cell viability assays upon JQ1 treatment. In these experiments, the prostate cancer cell line DU-145 seemed to be resistant against JQ1, further supporting a diminished KEAP/NRF2 axis in DU-145 cells.

BRD4 activates HMOX1 expression over specificity protein 1 (SP1) binding sites in the absence of stress. During our effort to clarify the regulatory role of BRD4 in the oxidative stress KEAP1/NRF2 response pathway, we have observed that a diminution of BRD4 leads to an increased production of the inducible HMOX1 after stimulation with CoPP. The situation in an uninduced state was different: A *BRD4* knockdown resulted in a decreased *HMOX1* level. To further analyze this discrepancy, we performed luciferase reporter assays in the absence of stress. *HMOX1* expression is regulated over several transcriptional regulatory elements and transcription factor binding sites and enhancer regions E1 and E2 located upstream of the *HMOX1* promoter region. We generated different luciferase constructs that either contained the enhancer region 1 in addition to a 2-kb region of the *HMOX1* promoter (E1-HMOX1-WT (wild type)) or fragments of different sizes of the promoter region alone (HMOX1-WT, HMOX1-367, HMOX1-228) (Figure 4a). An overexpression of NRF2 showed the expected increase of the luciferase signal with E1-HMOX1-WT but not with HMOX1-WT, confirming the transcriptional enhancement by
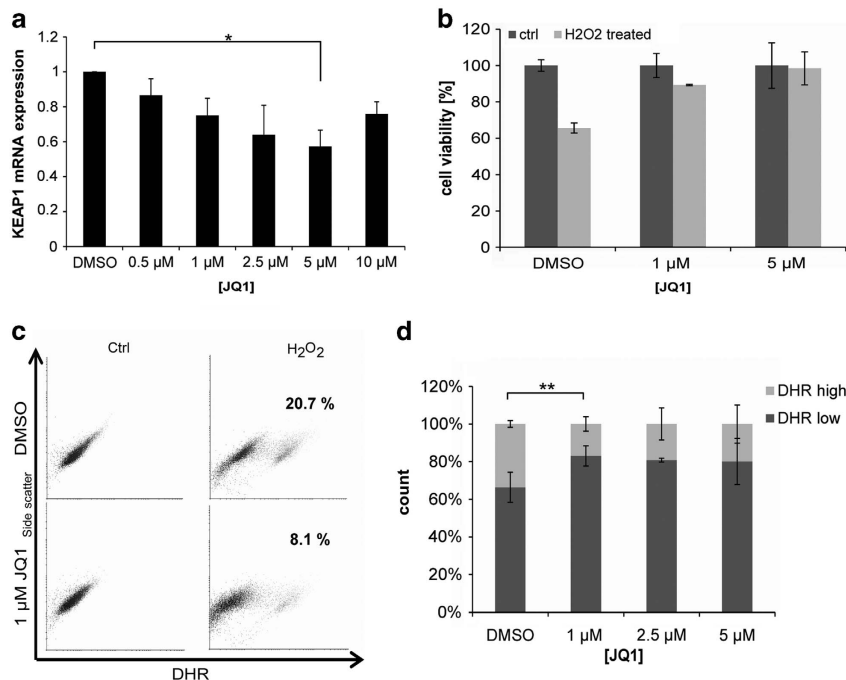
Figure 3 BRD4 inhibition decreases ROS and enhances cell survival under oxidative stress. (**a**) KEAP1 mRNA expression was analyzed in WI-38 cells after 72 h of JQ1 or DMSO treatment using qPCR. As a reference gene, β-tubulin was used. The results represent the averages of two independent experiments. (**b**) WI-38 cells were incubated with various concentrations of JQ1 for 72 h. Twenty-four hours before determination of cell viability, the cells were treated with 100 μM H_2O_2 for 30 min. (**c**) Determination of ROS in WI-38 cells. Cells were treated with 1 μM JQ1 or DMSO for 72 h. Four hours before detection, 1 mM H_2O_2 was used to stimulate ROS production. The intensity of intracellular ROS was measured using the fluorescence substrate DHR. Cells with high levels of ROS are shown in light grey, whereas the dark grey points represent cells with low ROS levels. Percentages indicate the relative amount of cells with high ROS levels. (**d**) Flow cytometry analysis using the Flowing Software 2 in cells treated with various concentrations of JQ1. The distribution of cells with high and low intensity of DHR was calculated and plotted as relative cell number. Low intensity of DHR represents low level of ROS, whereas high fluorescence indicates high level of ROS. (*P-values < 0.05 and **P-values < 0.01 according to two-tailed t-tests)
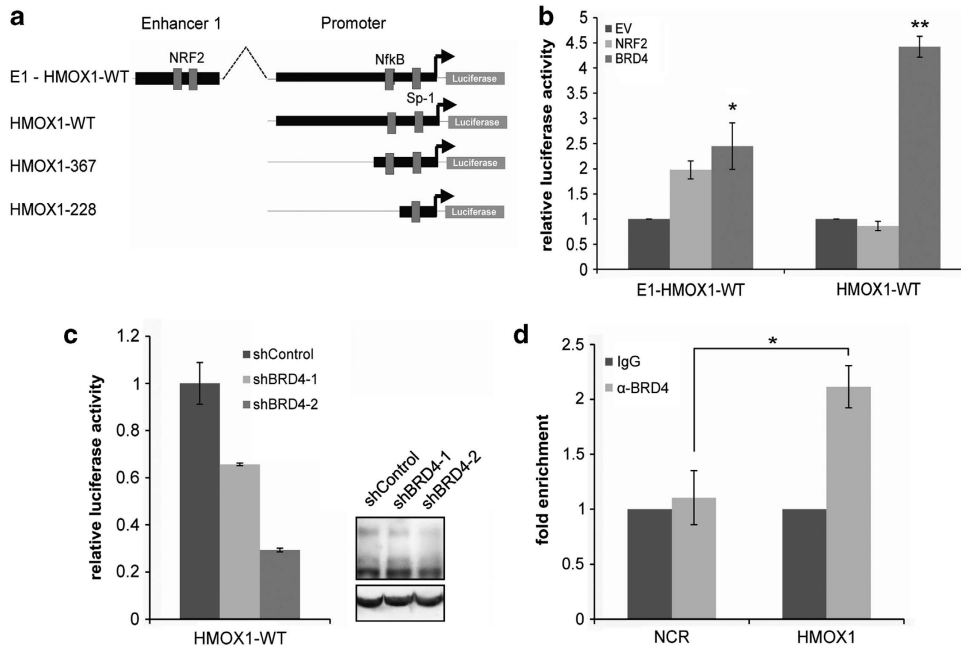
Figure 4 BRD4 regulates the transcription of HMOX1 in the absence of an inductor. (**a**) Schematics of the HMOX1 luciferase reporter constructs. (**b**) HMOX1 reporter assays with BRD4 and NRF2. BRD4 (pcDNA-BRD4-FL), NRF2 (pTL-FlagC-NRF2) expressing constructs or empty vectors (EV) were co-transfected with a luciferase reporter plasmid carrying the HMOX1 promoter either with (E1-HMOX1-WT) or without (HMOX1-WT) the first enhancer region of the HMOX1 gene. After 24 h, the cells were harvested for luciferase analysis. The promoter activity was normalized to EVs and co-transfected *renilla* luciferase activity. The results represent the averages of three independent experiments (*P-values < 0.05 and **P-values < 0.01 according to two-tailed t-tests). (**c**) HMOX1 reporter experiments with *BRD4* knockdown. HEK293T cells were co-transfected with either shBRD4-1, shBRD4-2 or shControl as control with the luciferase reporter carrying the HMOX1 promoter (HMOX1-WT). Seventy-two hours post transfection, the cells were harvested for measuring the luciferase activity or for western blot analysis. The activity was normalized to the *renilla* luciferase activity and transfections with an empty reporter construct. These results were confirmed by two biological replicates. Expression of BRD4 was measured with a western blot where tubulin was used as a loading control. (**d**) Binding of BRD4 to the HMOX1 promoter. ChIP analyses were performed with antibodies against BRD4 or with rabbit IgG as a negative control. The enrichment was analyzed with qPCRs for the promoter region of HMOX1 and an intergenic NCR. Values were normalized to the input and IgG controls (*P-values < 0.05 and **P-values < 0.01 according to two-tailed t-tests)

NRF2 through the enhancer regions (Figure 4b). Interestingly, a co-transfection with BRD4 only marginally increased the reporter activity of the E1-HMOX1-WT construct but instead showed an enhanced luciferase activity with the HMOX1-WT promoter construct. This suggests an additional transcriptional regulation mechanism of HMOX1 through BRD4 besides the KEAP1/NRF2 pathway. A *BRD4* knockdown significantly decreased the promoter activity of the HMOX1-WT construct to nearly 60% (Figure 4c). To investigate whether BRD4 directly activates the *HMOX1* transcription by direct association to the promoter, we performed a ChIP experiment with an α-BRD4 antibody. QPCR analyses showed that the *HMOX1* promoter, but not the NCR (non coding region), was > 2-fold increased in the BRD4 ChIP (Figure 4d).

To elucidate how BRD4 may regulate the HMOX1 promoter, we shortened the *HMOX1* promoter to curtail the regulatory elements. Using 367- and 228-bp long reporter constructs, we found the activating function of BRD4 independent of the NF-κB site (230–250 bp upstream of the TSS) (Figure 5a).[30] To identify BRD4 consensus-binding motifs, we used the binding regions identified from our ChIP-Seq experiments and performed bioinformatics analyses.[31] This resulted in the SP1-binding motif as one of our top candidates for BRD4 binding (Figure 5b, Supplementary Table S6).

We inserted SP1-binding site point mutations in the HMOX1-WT luciferase reporter plasmid and tested the promoter activity following BRD4 overexpression (Figure 5c). The mutation significantly abolished the transcriptional activation function of BRD4 by 50%.

Our experiments strongly suggest a regulation of HMOX1 by BRD4, even independent of the KEAP1/NRF2 pathway, through the direct association to the SP1-binding motif in the HMOX1 promoter.

Discussion

BRD4, an acetylated histone-binding protein, has been identified as an important factor for the regulation of primary response and interferon-stimulated gene expression.[30–34] Furthermore, BRD4 seems to have a complex role in the transcriptional program of different tumor entities. On the one hand, studies in colorectal and breast tumors suggest BRD4 to act as a tumor suppressor.[35,36] On the other hand, an overexpression of the short BRD4 isoform results in increased metastasis formation in breast tumors.[37] Becoming aware of BRD4 as a turnstile in tumor pathogenesis, understanding the molecular mechanism of BRD4 action can help to shed light on the complex de-regulated transcription machinery and to identify central cancer pathways. Here we used an integrated analysis of data from ChIP-Seq, RNA-Seq and gene
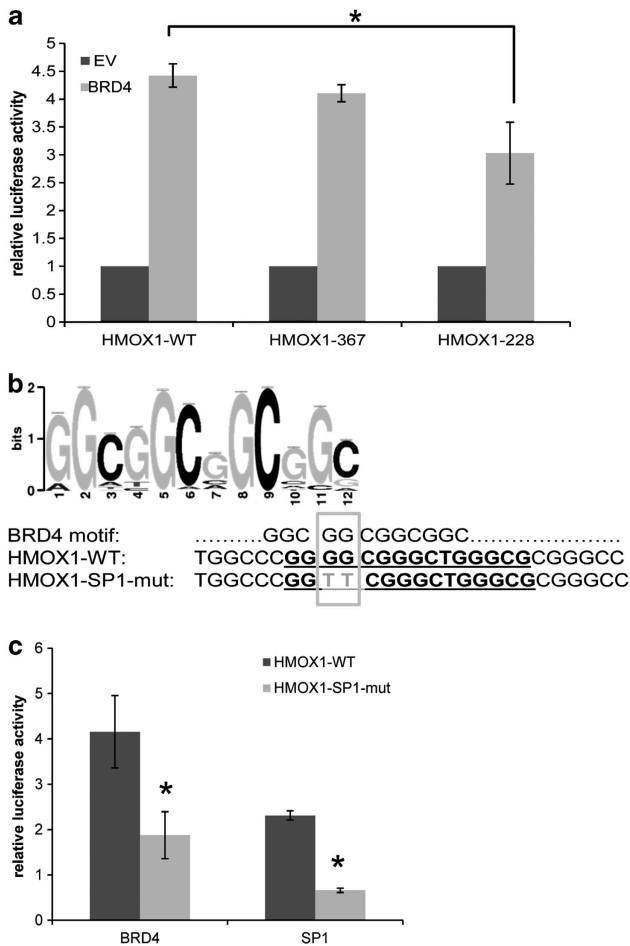
Figure 5 BRD4 regulates HMOX1 over the SP1-binding motif. (a) Mapping of the BRD4 activating region on the HMOX1 promoter. BRD4 (pcDNA-BRD4-FL) or empty vector (EV) were co-transfected with a luciferase construct carrying the full-length HMOX1 promoter (HMOX1-WT), a 367-bp long (HMOX1-367) or a 228-bp (HMOX1-228) long fragment of the HMOX1 promoter. Twenty-four hours post transfection, the cells were harvested, and the promoter activity was determined and normalized to the renilla luciferase and the EV signals. The results represent the averages of three independent experiments (*P-values < 0.05 according to two-tailed t-tests). (b) MEME analyses of BRD4 ChIP-Seq data. The binding matrix represents the identified BRD4 'binding motif' of the ChIP-Sequencing. Using the TOMTOM analysis tool, the SP1-binding motif was identified as one of the top known binding motifs associated with the BRD4-binding site (P-value: 0.00026, E-value: 0.2305; q-value: 0.1024). At the right, the SP1-binding site in the HMOX1 promoter (HMOX1-WT) and the used mutation (HMOX1-SP1-mut) are shown. (c) Reporter assays with wild-type (HMOX1-WT) or SP1-site-mutated (HMOX1-SP1-mut) HMOX1 reporter constructs. BRD4 and SP1 (pTL-FlagC-SP1) expressing constructs were co-transfected with either the HMOX1 wild-type promoter or with the SP1-binding site mutant. Twenty-four hours post transfection, the cells were harvested, and the promoter activity was determined and normalized to the renilla luciferase signal. The results represent the average of two independent experiments (*P-values < 0.05 according to two-tailed t-tests)

expression correlation analyses of primary prostate normal and tumor tissue samples to nominate 21 key BRD4 target genes in cancer.

Searching for possible common biological functions among these genes, we compared our list with the regions published by Loven et al.[18] and found for eight genes an enhancer region within the TSS. Interestingly, three of these genes are involved in the maintenance of physiological concentrations

of ROS: SESN3, HDAC6 and KEAP1. De-regulation of the intracellular ROS homeostasis can have fatal consequences for the organism, including the development of cancer, neurodegenerative diseases, rheumatoid arthritis, diabetes and inherited syndromes, such as Fanconi anemia.[38–40]

In the absence of stress, we noticed that BRD4 activates the HMOX1 promoter and regulates the HMOX1 expression over the SP1 promoter-binding sites (Figure 6a). Thus, BRD4 acts as a positive transcriptional activator of HMOX1, whereas BRD4 silencing results in decreased HMOX1 mRNA and protein expression as well as a reduced promoter activity (Figure 6b). This may be a mechanism for a fast fine-tuning of the cellular reactions towards small ROS deviations that do not activate the KEAP1/NRF2 oxidative stress response. However, we also identified KEAP1 as one of our top 21 BRD4 target genes. BRD4 binds to the KEAP1 promoter not only in normal but also in prostate cancer cells, highlighting KEAP1 as activating direct target for BRD4 in cancer.

Under CoPP treatment, and thus exertion of stress, NRF2 is significantly increased, which drives HMOX1 expression (Figure 6c). An additional BRD4 knockdown further enhances this mechanism by a downregulation of KEAP1 and a lack of NRF2 degradation (Figure 6d). The increase in HMOX1 goes along with an increased cell viability and a decreased amount of intracellular ROS under H_2O_2 stress and a decreased BRD4 function. Thus, under exertion of stress, BRD4's regulation of HMOX1 is mediated via the KEAP1/NRF2 pathway resulting in a counteraction of BRD4 and HMOX1 levels.

The KEAP1/NRF2 pathway is frequently disrupted by somatic mutations in tumors. NRF2-activating somatic mutations have been described in lung, head and neck, esophagus and skin cancers.[41,42] Mutations in NRF2 and KEAP1 are clustered within the KEAP1–NRF2-binding surface[43] but are mutually exclusive. KEAP1 mutations are found, next to abnormally increased DNA methylation, to impair KEAP1 function,[44–46] thus liberating NRF2 to the nucleus.[43] The increased activity of NRF2 in tumors, in turn, can promote ROS detoxification and tumorigenesis by conferring a more reducing intracellular environment.[47] HMOX1, the rate-limiting enzyme in the heme catabolism and part of the cellular defense against oxidative stress, is, similar to NRF2, recognized as resistance mechanism against tumor necrosis factor-induced cell death as shown in acute myeloic leukemia (AML).[48] Interestingly, in prostate cancer the block of the KEAP1/NRF2 pathway seems to be located even downstream of NRF2: We showed that in prostate cancer tissues, as well as in a subset of prostate cancer cell lines, HMOX1 is upregulated irrespective of NRF2. In this case, a treatment with JQ1 did not decrease ROS levels and did not lower cell viability as one would have expected owing to the high BRD4 levels in these cells. Similarly, Wyce et al.[49] found that IC_{50} values for the BET inhibitor I-BET762 for DU-145 cells were $> 3\,\mu M$, whereas for LNCaP cells $< 30\,nM$, supporting a therapy resistance of DU-145 cells. As our measurement of HMOX1 was done without exogenous stress, BRD4 might have bypassed the KEAP1/NRF2 pathway and directly regulated the HMOX1 promoter, as we have shown it in a cell culture model in absence of stress. As far as HMOX1 is concerned, Alaoui-Jamali et al.[50] described a significant
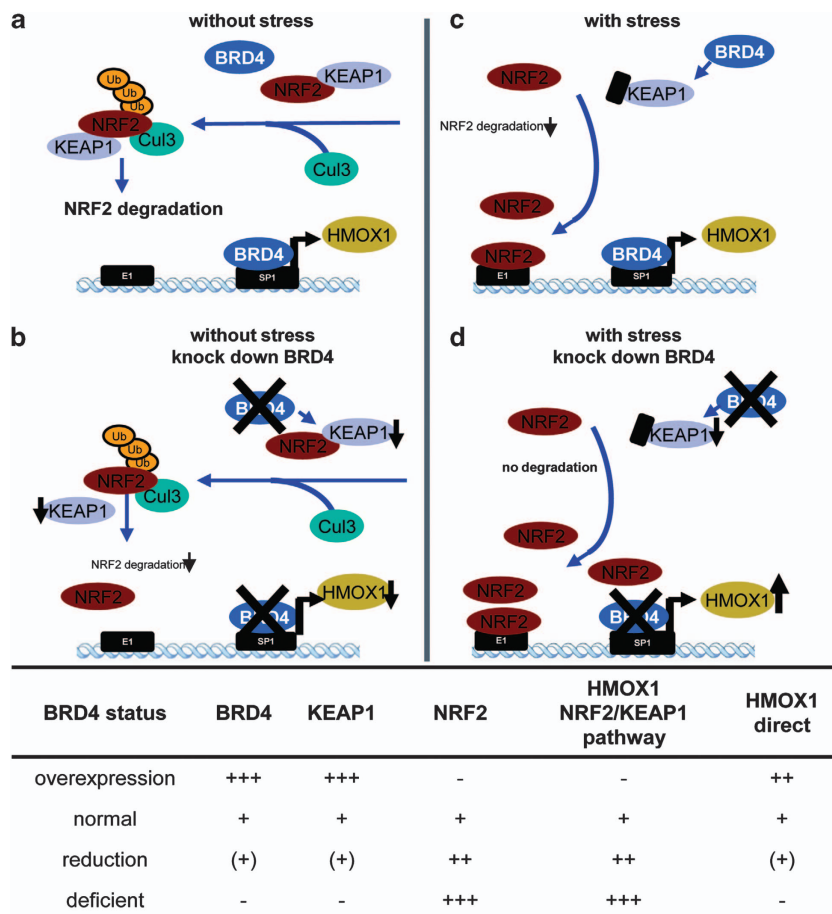
Figure 6 Schematics of the regulation of the *HMOX1* expression under normal (**a** and **b**) and stress conditions (**c** and **d**) and without (**a** and **c**) or with (**b** and **d**) *BRD4* knockdown. Under normal conditions, BRD4 directly activates the HMOX1 promoter over SP1-binding sites. In the presence of stress, *HMOX1* expression is mainly regulated over the NRF2/KEAP1 pathway where BRD4 regulates KEAP1. The table summarizes the regulation of HMOX1 under varying BRD4 concentrations

elevation of HMOX1 levels in hormone-refractory prostate cancer and silencing of the *HMOX1* gene or exposure to a small molecular HMOX1 inhibitor (OB-24) reduced cell proliferation, tumor growth and metastatic invasion. Having this all in mind, one may speculate that a high BRD4 level in combination with a high amount of HMOX1 might be an indicator for BET inhibitor resistance. *Vice versa*, the classic fields of application for BET inhibitors (e.g., JQ1, I-BET[29,51]) so far are AML, MLL, MM and melanoma. Abrogation of BRD4's function results in a delayed tumor progression, survival benefits, loss of stem cell characteristics and a reduction of MYC oncogene expression. Searching the Oncomine database, we found for AML and MM significantly decreased *HMOX1* expressions. Thus, the effective treatment of AML and MM patients with BET inhibitors may – at least partly – be supported by low HMOX1 levels.

Taken together, our data provide new insight into the transcriptional regulatory network of BRD4 as it nominates BRD4 as key mediator of KEAP1 in the oxidative stress response and to directly target SP1-binding sites in the *HMOX1* promoter (Figure 6). In prostate tumors, these regulatory mechanisms appear to be disturbed. The increased *BRD4* and *KEAP1* expression in prostate cancer does not go along with decreased *HMOX1* levels. In contrast,

HMOX1 seems to be upregulated independently of the KEAP1–NRF2 pathway (Figure 6), suggesting that the strong increase in *BRD4* may, over a direct regulation of the *HMOX1* promoter, counteract the downregulation of HMOX1 via KEAP1-NRF2. The two-sided regulatory mechanism of BRD4 may prevent tumor cells from a loss of HMOX1, an increase of ROS and promote cell survival. As outlined above, further studies of the BRD4 transcriptional network and the cooperation between BRD4, KEAP1, NRF2 and NRF2 target genes as transcriptional regulators in prostate cancer have the potential to elucidate important druggable oncogenic dependencies.

Materials and Methods
Plasmids, RNA interference, site-directed mutagenesis and antibodies. The BRD4 shRNA knockdown vectors (shBRD4-1, shBRD4-2) and the control vector have been described previously in Schweiger *et al.*[52] The siRNA-BRD4-pool (siBRD4) as well as the non-targeting control pool (siControl) were purchased from Thermo Scientific (Schwerte, Germany). The pcDNA4c-plasmid containing the full-length human BRD4 has been described previously in You *et al.*[53] NRF2 and SP1 were cloned into the pTLFlagC vector system using the following primers:

NRF2-fw: 5′-GAATGCGGCCGCCATGGCATAAAGCCCTACAGC-3′,
NRF2-rev: 5′-TTACGCGTCGACAGAGCGTCCGCAACCCGACA-3′,
SP1-fw: 5′-TTACGCGTCGACAAGCGACCAAGATCACTCCAT-3′, and

SP1-rev: 5′-GAATGCGGCCGCTCAGAAGCCATTGCCACTGATA-3′.

For the luciferase reporter assay, the HMOX1 promoter was cloned into the pGL3-basic vector from Promega (Mannheim, Germany). The following primers were used for cloning the HMOX1 promoter fragments:

HMOX1-WT-fw: 5′-TTTAGATCTCACCAGACCCAGACAGATTTACCT-3′,
HMOX1-367-fw: 5′-TTTAGATCTGAGCCTGCAGCTTCTCAGATTT-3′,
HMOX1-228-fw: 5′-TTTAGATCTTATGACTGCTCCTCTCCACCCC-3′, and
HMOX1-rev: 5′-TTTAAGCTTGTGCTGGGCTCGTTCGTGCTGGCT-3′.

The enhancer region E1 was cloned into the BamH1 and SalI restriction sites in the pGL3-basic vector using the primers HMOX1-E1fw: 5′-ACAATTGGCCCAGTCTATGG-3′ and HMOX1-E1rev: 5′-GGAGTTCAAGACCAGCCTGA-3′. The SP1-binding site mutation in the HMOX1 promoter was created with the QuikChange II Site-Directed Mutagenesis Kits (Agilent, Santa Clara, CA, USA) according to the manufacturer's protocol.

The following antibodies were used: rabbit polyclonal BRD4 antibody (ab75898, Abcam, Cambridge, UK), mouse monoclonal HMOX1 antibody (ab13243, Abcam), NRF2 (sc13032, sc722, Santa Cruz Biotechnology, Heidelberg, Germany), KEAP1 (K2769, Sigma-Aldrich, Taufkirchen, Germany), alpha-tubulin (T9026, Sigma-Aldrich), and beta-actin (Cell Signaling, Leiden, Netherlands).

Luciferase reporter assay. The luciferase construct or the corresponding negative control (pGL3-basic vector) were transfected together with a BRD4, NRF2 or SP1 expression construct or shRNA plasmids. Luciferase activities were measured 24 h after transfection for overexpression or 72 h after knockdown approaches according to the manufacturer's protocol (Dual-Luciferase Reporter Assay System from Promega). Luciferase activities were normalized to the luciferase activity of a co-transfected *renilla* expression plasmid.

Cell culture, CoPP treatment and transfection. Cells were cultivated at 37 °C with 5% CO$_2$ in their specific cell culture medium (Hek293T and DU-145: Dulbecco's Modified Eagle's Medium, WI-38: Minimal essential Medium containing 10% fetal calf serum, 2 mM L-glutamine and 100 U penicillin/streptomycin and RWPE-1: keratinocyte serum-free medium supplemented with EGF and BPE). Cells were treated with 20–100 μM CoPP (dissolved in DMSO) for 4–14 h and with various concentrations of JQ1 (Cayman Chemical: 1268524-70-4, Ann Arbor, MI, USA) for 72 h. Plasmids were transfected into the cells using X-treme gene 9 transfection reagent (Roche, Penzberg, Germany) and siRNA using HiPerFect transfection reagent (Qiagen, Hilden, Germany).

Cell viability assay. Cell viability was measured using the Alamar Blue reagent from Life Technologies (Darmstadt, Germany). Cells were seeded in 96-well plates and treated with siRNAs or JQ1 inhibitor. After incubation for 72 h at 37 °C, 10 μl of Alamar Blue cell viability reagent was added according to manufacturer's instructions, and the resulting fluorescence intensity was read on the fluorescence spectrometer LS55 (Perkin Elmer, Waltham, MA, USA).

ROS detection using flow cytomery. Cells were seeded in 12-well plates and treated with siRNAs or JQ1 inhibitor at various concentrations. After incubation for 72 h, 10 μM DHR or 10 μM DHR + 1 mM H$_2$O$_2$ was added for additional 4 h to determine the levels of oxidative stress products. The absorbance of the green fluorescent rhodamine 123 was measured using an ACCURI C6 cytometer and analyzed with the Flowing Software 2 (BD Bioscience, San Jose, CA, USA).

Protein extraction, western blot analysis and immunofluorescence. Cells were harvested and resuspended in 300 μl lysis buffer A (10 mM Hepes-KOH (pH 7.4), 10 mM NaCl, 1 mM DTT, 3 mM Mg$_2$Cl and protease inhibitor cocktail (Roche)). Cells were incubated for 10 min on ice before passaging through a needle 10 times. NaCl was added to a final concentration of 300 mM, and the lysate was rotated at 4 °C for 20 min. After centrifugation for 5 min at 2500 × *g* at 4 °C, the supernatant was transferred to a new tube. The pellet containing insoluble proteins was resuspended in 300-μl lysis buffer B (10 mM Hepes-KOH (pH 7.4), 300 mM NaCl, 1 mM DTT, 20 mM Mg$_2$Cl, 0.2 U DNase and Protease Inhibitor cocktail (Roche)) and incubated for 30 min at 37 °C. The extract was centrifuged at 2500 × *g* at 4 °C for 5 min, and the supernatant was combined with the soluble protein fraction. Protein extracts (30 μg) were separated on a 10% SDS gel, transferred to a polyvinylidene difluoride (PVDF) membrane and immunoblot analyses were performed with the aforementioned antibodies.

For immunofluorescence, cells were seeded on cover slips and cultivated at 37 °C. After treatment, cells were fixed with 100% methanol at −20 °C and incubated with antibodies against NRF2 (1 : 100 in PBS) overnight at 4 °C followed by an incubation with Alexa-fluor 594-labeled secondary antibody. Analysis of subcellular localizations was performed using a confocal fluorescence microscope (LSM 510 meta, Zeiss, Jena, Germany), and image analysis was carried out with the Axio vision software (Zeiss).

ChIP and illumina sequencing (ChIP-Seq). ChIP was done according to the protocol of Dahl *et al.*[54] Briefly, immediately before harvesting the cells sodium butyrate (Sigma-Aldrich) was added to the cell culture medium to a final concentration of 20 mM and mixed gently. The cells were harvested by trypsinization and cross-linked with 1% (v/v) formaldehyde for 10 min at room temperature. The cross-link reaction was stopped by adding glycine to a final concentration of 125 mM for 5 min. Cells were lysed with lysis buffer (50 mM Tris-HCl, 10 mM EDTA, 1% SDS, protease inhibitor cocktail and 20 mM sodium butyrate). The chromatin was sheared by sonication to a DNA fragment size of 200–600 bp and precipitated by centrifugation at 12 000 × *g* at 4 °C for 10 min. For immunoprecipitations, 5 μg of each antibody or of a rabbit immunglobulin G (IgG) control were incubated overnight with the sheared DNA. The next day, 50 μl protein G Dynabeads (Life Technologies) were added and incubated for 4 h at 4 °C. The antibody/chromatin/beads complexes were washed four times with RIPA buffer (10 mM Tris-HCl, 1 mM EDTA, 0.5 mM EGTA, 1% Triton-X100, 0,1% SDS, 0,1% sodium-deoxycholate and 140 mM NaCl) and once with TE-buffer (10 mM Tris-HCl, 10 mM EDTA). DNA was incubated with elution buffer (20 mM Tris-HCl, 5 mM EDTA, 20 mM sodium butyrate, 50 mM NaCl) containing 50 μg/ml proteinase K at 68 °C for 2 h. DNA was purified using the Qiagen MinElute columns (Qiagen). In all, 300 pg of ChIP and input DNA were analyzed using qPCR with the following primers:

HMOX1_Prom_fw: 5′-GGATTCCAGCAGGTGACATT-3′ and HMOX1_Prom_rev: 5′-GTGGGCAACATCAGGAACTT-3′;
HMOX1_E1_fw: 5′-GAAGGCGGATTTTGCTAGATTT-3′ and HMOX1_E1_rev: 5′-CTCCTGCCTACCATTAAAGCTG-3′;
KEAP1_Prom_fw: 5′-GAAAGGAGCGGCGATTCTC-3′ and KEAP1_Prom_rev: 5′-TGGAAGGGACAGTGAGAAGG-3′;
HDAC6_Prom_fw: 5′-GCCAGTGTTTCCTGTGTACC-3′ and HDAC6_Prom_rev: 5′-GTTGCCACTGGACGTTGG-3′;
SESN3_Prom_fw: 5′-CCCTGCTCAGAAAGGAAGGT-3′ and SESN3_Prom_rev: 5′-TGGACGCTAAAACCCTGACT-3′;
MAPK3_Prom_fw: 5′-CAGGCTGGAGTGTAGTGGTG-3′ and MAPK3_Prom_rev: 5′-CACTCGTAGTCCCAGCTCTT-3′; and
VIM_Prom_fw: 5′-GAAGAGCGAGAGGAGACCAG-3′ and VIM_Prom_rev: 5′-CTCCCAGATCACGATTGCAC-3′.

As a negative control (NCR), the following primers were used:
NCR-fw: 5′-TGCTGTTACTTTTTACAGGGAGTT-3′ and NCR-rev: 5′-TTTGAGC AAAAATGTTGAAAACAA-3′.

The relative enrichment towards the IgG control was calculated using the %Input method previously described.[55] Sequencing libraries were prepared according to the Illumina's ChIP-Seq Sample Prep Kit and analyzed on the Illumina Genome Analyzer IIx (Illumina, San Diego, CA, USA) (Supplementary Table S7).

RNA-Sequencing (RNA-Seq) and qPCR. Total RNA was purified using the RNA MicroPrep Kit (Zymo Research, Irvine, CA, USA). Complementary DNA was generated using SuperScript II Reverse Transcriptase (Life Technologies) according to the manufacturer's instructions. The relative expression was calculated using the $\Delta\Delta Ct$ method. The following primers were used for qPCRs:

BRD4-fw: 5′-AACCTGGCGTTTCCACGGTA-3′ and
BRD4-rev: 5′-GCCTGCACAGGAGGAGGATT-3′,
HMOX1-fw: 5′-AGACGGCTTCAAGCTGGTGAT-3′ and
HMOX1-rev: 5′-CCTTGTTGCGCTCAATCTCCT-3′,
NRF2-fw: 5′-TACTCCCAGGTTGCCCACAT-3′ and
NRF2-rev: 5′-AATGTCTGCGCCAAAAGC-3′,
KEAP1-fw: 5′-TGGCCAAGCAAGAGGAGTTC-3′ and
KEAP1-rev: 5′-GGCTGATGAGGGTCACCAGTT-3′ and
TUBB-fw: 5′-GCTGGACCGCATCTCGTGTA-3′ and
TUBB-rev: 5′-CAGAGTCCATGGTCCCAGGTT-3′.

Library preparations were performed following the instructions of the TrueSeq RNA Sample Preparation Kit (Illumina), and sequencing was performed on the Illumina HighSeq 2500 (Supplementary Table S7). Validation of the RNA-Seq data

was performed with qPCR experiments and resulted in Pearson's correlation coefficients of 0.86 (Supplementary Figure S2b).

Bioinformatics and statistical analysis

Primary sequencing data analysis: Sequences were generated using Illumina's HiSeq 2500 instrument. Fastq files were obtained after demultiplexing using Illuminas CASAVA v1.8.2 pipeline with default parameters. All data have been deposited in NCBI's Gene Expression Omnibus[56] and are accessible through GEO Series accession number GSE50491.

Secondary analysis: Reads were mapped against the human genome GRCh37/hg19 using bwa v0.5.9-r16 with default parameters.

RNA-Seq expression analysis: Exon read coverages were obtained with coverageBed v2.17.0 using exon coordinates of the Ensembl database v63. Transcript counts were generated by summing read counts across all exons of a given transcript.

Expression changes were calculated as log2(ratios) of the read counts $+1$ read per transcript for two investigated conditions, and ratios were normalized against the median ratio of each condition.

ChIP-Seq analysis: Bam files from bwa alignments were used as input information and peaks were called with MACS v1.4[57] using an enrichment ratio against the background of 5–15 to build the model ($m = 5,15$). PeakSplitter v1[58] was used with default parameters to call the subpeaks. Obtained subpeaks were subsequently annotated to TSS. In more detail, a subpeak was associated to a promoter if at least one base of the identified peak range was within 500 bp upstream of a TSS. We used MEME v4.6.1[31] with the parameters -mod zoops -text -dna -revcomp -nostatus -nmotifs 10 -minw 8 -maxw 12 -maxsize 15 000 000 to search for enriched sequence motifs (zero or one motif per peak) in a window of 300 bp around the subpeak summit. Obtained sequence motifs were annotated to known transcription factor-binding sites with TOMTOM[31] using E-value or q-value cutoffs of $E < 0.5$ or $q < 0.1$.

Microarray expression analysis: Expression data of prostate cancer biopsies were obtained as quantile-normalized values from the publication by Brase et al.[24] GEO database (NCBI, GEO, GSE29079). For the determination of BRD4 expression levels, we used the core probe set of the Affymetrix human exon 1.0 ST array (Affymetrix, Santa Clara, CA, USA). The BRD4 core probes are located at the very C-terminus of the long BRD4 isoform.

Conflict of Interest

The authors declare no conflict of interest.

1. Schreck R, Rieber P, Baeuerle PA. Reactive oxygen intermediates as apparently widely used messengers in the activation of the NF-kappa B transcription factor and HIV-1. *EMBO J* 1991; **10**: 2247–2258.
2. McMahon M, Itoh K, Yamamoto M, Hayes JD. Keap1-dependent proteasomal degradation of transcription factor Nrf2 contributes to the negative regulation of antioxidant response element-driven gene expression. *J Biol Chem* 2003; **278**: 21592–21600.
3. Alam J, Cook JL. Transcriptional regulation of the heme oxygenase-1 gene via the stress response element pathway. *Curr Pharm Des* 2003; **9**: 2499–2511.
4. Kobayashi A, Ohta T, Yamamoto M. Unique function of the Nrf2-Keap1 pathway in the inducible expression of antioxidant and detoxifying enzymes. *Methods Enzymol* 2004; **378**: 273–286.
5. Itoh K, Wakabayashi N, Katoh Y, Ishii T, O'Connor T, Yamamoto M. Keap1 regulates both cytoplasmic-nuclear shuttling and degradation of Nrf2 in response to electrophiles. *Genes Cells* 2003; **8**: 379–391.
6. Zhang DD, Hannink M. Distinct cysteine residues in Keap1 are required for Keap1-dependent ubiquitination of Nrf2 and for stabilization of Nrf2 by chemopreventive agents and oxidative stress. *Mol Cell Biol* 2003; **23**: 8137–8151.
7. Ikeda H, Serria MS, Kakizaki I, Hatayama I, Satoh K, Tsuchida S et al. Activation of mouse Pi-class glutathione S-transferase gene by Nrf2(NF-E2-related factor 2) and androgen. *Biochem J* 2002; **364**(Pt 2): 563–570.
8. McMahon M, Itoh K, Yamamoto M, Chanas SA, Henderson CJ, McLellan LI et al. The Cap'n'Collar basic leucine zipper transcription factor Nrf2 (NF-E2 p45-related factor 2) controls both constitutive and inducible expression of intestinal detoxification and glutathione biosynthetic enzymes. *Cancer Res* 2001; **61**: 3299–3307.
9. Alam J, Stewart D, Touchard C, Boinapally S, Choi AM, Cook JL. Nrf2, a Cap'n'Collar transcription factor, regulates induction of the heme oxygenase-1 gene. *J Biol Chem* 1999; **274**: 26071–26078.
10. Singh A, Misra V, Thimmulappa RK, Lee H, Ames S, Hoque MO et al. Dysfunctional KEAP1-NRF2 interaction in non-small-cell lung cancer. *PLoS Med* 2006; **3**: e420.
11. Ohta T, Iijima K, Miyamoto M, Nakahara I, Tanaka H, Ohtsuji M et al. Loss of Keap1 function activates Nrf2 and provides advantages for lung cancer cell growth. *Cancer Res* 2008; **68**: 1303–1309.
12. Cancer Genome Atlas Research N. Comprehensive genomic characterization of squamous cell lung cancers. *Nature* 2012; **489**: 519–525.
13. Schweiger MR, You J, Howley PM. Bromodomain protein 4 mediates the papillomavirus E2 transcriptional activation function. *J Virol* 2006; **80**: 4276–4285.
14. Jang MK, Mochizuki K, Zhou M, Jeong HS, Brady JN, Ozato K. The bromodomain protein Brd4 is a positive regulatory component of P-TEFb and stimulates RNA polymerase II-dependent transcription. *Mol Cell* 2005; **19**: 523–534.
15. Wu SY, Chiang CM. The double bromodomain-containing chromatin adaptor Brd4 and transcriptional regulation. *J Biol Chem* 2007; **282**: 13141–13145.
16. Zhang W, Prakash C, Sum C, Gong Y, Li Y, Kwok JJ et al. Bromodomain-containing protein 4 (BRD4) regulates RNA polymerase II serine 2 phosphorylation in human CD4 + T cells. *J Biol Chem* 2012; **287**: 43137–43155.
17. Devaiah BN, Lewis BA, Cherman N, Hewitt MC, Albrecht BK, Robey PG et al. BRD4 is an atypical kinase that phosphorylates serine2 of the RNA polymerase II carboxy-terminal domain. *Proc Natl Acad Sci USA* 2012; **109**: 6927–6932.
18. Loven J, Hoke HA, Lin CY, Lau A, Orlando DA, Vakoc CR et al. Selective inhibition of tumor oncogenes by disruption of super-enhancers. *Cell* 2013; **153**: 320–334.
19. Whyte WA, Orlando DA, Hnisz D, Abraham BJ, Lin CY, Kagey MH et al. Master transcription factors and mediator establish super-enhancers at key cell identity genes. *Cell* 2013; **153**: 307–319.
20. Lockwood WW, Zejnullahu K, Bradner JE, Varmus H. Sensitivity of human lung adenocarcinoma cell lines to targeted inhibition of BET epigenetic signaling proteins. *Proc Natl Acad Sci USA* 2012; **109**: 19408–19413.
21. Zuber J, Shi J, Wang E, Rappaport AR, Herrmann H, Sison EA et al. RNAi screen identifies Brd4 as a therapeutic target in acute myeloid leukaemia. *Nature* 2011; **478**: 524–528.
22. Dawson MA, Prinjha RK, Dittmann A, Giotopoulos G, Bantscheff M, Chan WI et al. Inhibition of BET recruitment to chromatin as an effective treatment for MLL-fusion leukaemia. *Nature* 2011; **478**: 529–533.
23. Segura MF, Fontanals-Cirera B, Gaziel-Sovran A, Guijarro MV, Hanniford D, Zhang G et al. BRD4 sustains proliferation and represents a new target for epigenetic therapy in melanoma. *Cancer Res* 2013; **73**: 6264–6276.
24. Brase JC, Johannes M, Mannsperger H, Falth M, Metzger J, Kacprzyk LA et al. TMPRSS2-ERG -specific transcriptional modulation is associated with prostate cancer biomarkers and TGF-beta signaling. *BMC Cancer* 2011; **11**: 507.
25. Yoo NJ, Kim HR, Kim YR, An CH, Lee SH. Somatic mutations of the KEAP1 gene in common solid cancers. *Histopathology* 2012; **60**: 943–952.
26. Karve TM, Rosen EM. B-cell translocation gene 2 (BTG2) stimulates cellular antioxidant defenses through the antioxidant transcription factor NFE2L2 in human mammary epithelial cells. *J Biol Chem* 2012; **287**: 31503–31514.
27. Rangasamy T, Guo J, Mitzner WA, Roman J, Singh A, Fryer AD et al. Disruption of Nrf2 enhances susceptibility to severe airway inflammation and asthma in mice. *J Exp Med* 2005; **202**: 47–59.
28. Alam J, Cai J, Smith A. Isolation and characterization of the mouse heme oxygenase-1 gene. Distal 5' sequences are required for induction by heme or heavy metals. *J Biol Chem* 1994; **269**: 1001–1009.
29. Filippakopoulos P, Qi J, Picaud S, Shen Y, Smith WB, Fedorov O et al. Selective inhibition of BET bromodomains. *Nature* 2010; **468**: 1067–1073.
30. Huang B, Yang XD, Zhou MM, Ozato K, Chen LF. Brd4 coactivates transcriptional activation of NF-kappaB via specific binding to acetylated RelA. *Mol Cell Biol* 2009; **29**: 1375–1387.
31. Bailey TL, Boden M, Buske FA, Frith M, Grant CE, Clementi L et al. MEME SUITE: tools for motif discovery and searching. *Nucleic Acids Res* 2009; **37**(Web Server issue): W202–W208.
32. Patel MC, Debrosse M, Smith M, Dey A, Huynh W, Sarai N et al. BRD4 coordinates recruitment of pause-release factor P-TEFb and the pausing complex NELF/DSIF to regulate transcription elongation of interferon stimulated genes. *Mol Cell Biol* 2013; **33**: 2497–2507.
33. Fowler T, Sen R, Roy AL. Regulation of primary response genes. *Mol Cell* 2011; **44**: 348–360.
34. Hargreaves DC, Horng T, Medzhitov R. Control of inducible gene expression by signal-dependent transcriptional elongation. *Cell* 2009; **138**: 129–145.

35. Crawford NP, Alsarraj J, Lukes L, Walker RC, Officewala JS, Yang HH et al. Bromodomain 4 activation predicts breast cancer survival. Proc Natl Acad Sci USA 2008; 105: 6380–6385.

36. Rodriguez RM, Huidobro C, Urdinguio RG, Mangas C, Soldevilla B, Dominguez G et al. Aberrant epigenetic regulation of bromodomain BRD4 in human colon cancer. J Mol Med (Berl) 2012; 90: 587–595.

37. Alsarraj J, Walker RC, Webster JD, Geiger TR, Crawford NP, Simpson RM et al. Deletion of the proline-rich region of the murine metastasis susceptibility gene Brd4 promotes epithelial-to-mesenchymal transition- and stem cell-like conversion. Cancer Res 2011; 71: 3121–3131.

38. Winyard PG, Moody CJ, Jacob C. Oxidative activation of antioxidant defence. Trends Biochem Sci 2005; 30: 453–461.

39. Ruppitsch W, Meisslitzer C, Weirich-Schwaiger H, Klocker H, Scheidereit C, Schweiger M et al. The role of oxygen metabolism for the pathological phenotype of Fanconi anemia. Hum Genet 1997; 99: 710–719.

40. Kontou M, Hirsch-Kauffmann M, Schweiger M. Impaired synthesis of heme oxygenase-1 in Fanconi anemia cells can be rescued by transfection of Fanconi wild-type cDNA. Biol Chem 2008; 389: 1327–1332.

41. Shibata T, Ohta T, Tong KI, Kokubu A, Odogawa R, Tsuta K et al. Cancer related mutations in NRF2 impair its recognition by Keap1-Cul3 E3 ligase and promote malignancy. Proc Natl Acad Sci USA 2008; 105: 13568–13573.

42. Kimm H, Kim S, Jee SH. The independent effects of cigarette smoking, alcohol consumption, and serum aspartate aminotransferase on the alanine aminotransferase ratio in korean men for the risk for esophageal cancer. Yonsei Med J 2010; 51: 310–317.

43. Taguchi K, Motohashi H, Yamamoto M. Molecular mechanisms of the Keap1-Nrf2 pathway in stress response and cancer evolution. Genes Cells 2011; 16: 123–140.

44. Barbano R, Muscarella LA, Pasculli B, Valori VM, Fontana A, Coco M et al. Aberrant Keap1 methylation in breast cancer and association with clinicopathological features. Epigenetics 2013; 8: 105–112.

45. Hanada N, Takahata T, Zhou Q, Ye X, Sun R, Itoh J et al. Methylation of the KEAP1 gene promoter region in human colorectal cancer. BMC Cancer 2012; 12: 66.

46. Muscarella LA, Barbano R, D'Angelo V, Copetti M, Coco M, Balsamo T et al. Regulation of KEAP1 expression by promoter methylation in malignant gliomas and association with patient's outcome. Epigenetics 2011; 6: 317–325.

47. DeNicola GM, Karreth FA, Humpton TJ, Gopinathan A, Wei C, Frese K et al. Oncogene-induced Nrf2 transcription promotes ROS detoxification and tumorigenesis. Nature 2011; 475: 106–109.

48. Rushworth SA, MacEwan DJ. HO-1 underlies resistance of AML cells to TNF-induced apoptosis. Blood 2008; 111: 3793–3801.

49. Wyce A, Degenhardt Y, Bai Y, Le B, Korenchuk S, Crouthame MC et al. Inhibition of BET bromodomain proteins as a therapeutic approach in prostate cancer. Oncotarget 2013; 4: 2419–2429.

50. Alaoui-Jamali MA, Bismar TA, Gupta A, Szarek WA, Su J, Song W et al. A novel experimental heme oxygenase-1-targeted therapy for hormone-refractory prostate cancer. Cancer Res 2009; 69: 8017–8024.

51. Nicodeme E, Jeffrey KL, Schaefer U, Beinke S, Dewell S, Chung CW et al. Suppression of inflammation by a synthetic histone mimic. Nature 2010; 468: 1119–1123.

52. Schweiger MR, Ottinger M, You J, Howley PM. Brd4-independent transcriptional repression function of the papillomavirus e2 proteins. J Virol 2007; 81: 9612–9622.

53. You J, Croyle JL, Nishimura A, Ozato K, Howley PM. Interaction of the bovine papillomavirus E2 protein with Brd4 tethers the viral DNA to host mitotic chromosomes. Cell 2004; 117: 349–360.

54. Dahl JA, Collas P. A quick and quantitative chromatin immunoprecipitation assay for small cell samples. Front Biosci 2007; 12: 4925–4931.

55. Mochizuki K, Nishiyama A, Jang MK, Dey A, Ghosh A, Tamura T et al. The bromodomain protein Brd4 stimulates G1 gene transcription and promotes progression to S phase. J Biol Chem 2008; 283: 9040–9048.

56. Edgar R, Domrachev M, Lash AE. Gene Expression Omnibus: NCBI gene expression and hybridization array data repository. Nucleic Acids Res 2002; 30: 207–210.

57. Zhang Y, Liu T, Meyer CA, Eeckhoute J, Johnson DS, Bernstein BE et al. Model-based analysis of ChIP-Seq (MACS). Genome Biol 2008; 9: R137.

58. Salmon-Divon M, Dvinge H, Tammoja K, Bertone P. PeakAnalyzer: genome-wide annotation of chromatin binding and modification loci. BMC Bioinformatics 2010; 11: 415.

59. Borno ST, Fischer A, Kerick M, Falth M, Laible M, Brase JC et al. Genome-wide DNA methylation events in TMPRSS2-ERG fusion-negative prostate cancers implicate an EZH2-dependent mechanism with miR-26a hypermethylation. Cancer Discov 2012; 2: 1024–1035.

Supplementary Information accompanies this paper on Cell Death and Disease website (http://www.nature.com/cddis)